A New Method to Solve Film Model for CO_2 Absorption with Aqueous Solution of N-Methyldiethanolamine

ZHONG Zhantie(钟战铁), **LI Wei**(李伟), **SHI Yao**(施耀)*, **HE Feng**(何锋) **and ZHOU Minghua**(周明华)
Department of Environmental Engineering, Zhejiang University, Hangzhou 310027, China

Abstract The shooting method and the difference method are used for numerical simulation of CO_2 absorption with aqueous solution of methyldiethanolamine (MDEA). It is demonstrated that these methods are available for the steady-state model, which may be expressed as a set of differential algebraic equations (DAEs) with two-point boundary values. This method makes it possible not only to obtain the concentration profiles for MDEA system, but also to reveal the effect of CO_2 interfacial concentration on the enhancement factor. With this numerical simulation, the mass transfer process with multicomponent diffusion and reactions can be better understood.
Keywords film model, numerical simulation, carbon dioxide, methyldiethanolamine
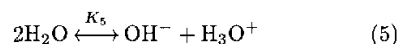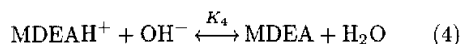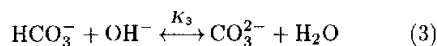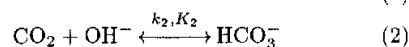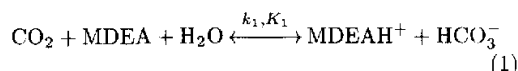
1 INTRODUCTION

Absorption with chemical reaction is widely used in industry, such as CO_2 absorption with alkanolamines, and H_2S removal by alkali solution. It is necessary to predict the effect of chemical reaction on absorption process by using models of rate of mass transfer, which may take the forms of the well-known film, penetration or surface renewal theories. However, the models for general reaction schemes are coupled, nonlinear ordinary or partial differential equations. Since it is difficult to get their analytical solutions, numerical solutions are unusually considered. Perry and Pigford[1], Cornelisser *et al.*[2] and Versteeg *et al.*[3] studied the numerical techniques for the models involving one reaction scheme. Glasscock and Rochelle[4], Hagewiesche *et al.*[5] and Rinker *et al.*[6] obtained the solutions for multicomponent diffusion and reactions by using the code DASSL[7] and DDASSL[8]. However, these codes have some restrictions. For example, they are only available for the initial-value problems, and the rigorous form of the equations are required[8].

CO_2 absorption with aqueous solution of N-methyldiethanolamine (MDEA) is a typical mass transfer process with multi-reaction. Based on the film theory, this process can be expressed as a set of differential algebraic equations (DAEs) with two-point boundary values. Although the film model is considered a simple one, it is not easy to solve the problem. In this paper two different numerical techniques are used to solve the problem with the purpose of obtaining available methods for this kind of mass transfer rate model.

2 MODEL OF CO_2 ABSORPTION WITH MDEA

When CO_2 is absorbed into an aqueous solution of a tertiary alkanolamine, MDEA, the following reactions may occur[5]

$$CO_2 + MDEA + H_2O \xrightleftharpoons{k_1, K_1} MDEAH^+ + HCO_3^- \tag{1}$$

$$CO_2 + OH^- \xrightleftharpoons{k_2, K_2} HCO_3^- \tag{2}$$

$$HCO_3^- + OH^- \xrightleftharpoons{K_3} CO_3^{2-} + H_2O \tag{3}$$

$$MDEAH^+ + OH^- \xrightleftharpoons{K_4} MDEA + H_2O \tag{4}$$

$$2H_2O \xrightleftharpoons{K_5} OH^- + H_3O^+ \tag{5}$$

Since the concentration of hydronium ion is very low under the condition of simulation, reaction(5) can be neglected [4]. For convenience, the concentrations of chemical species are represented as: $c_1 = [CO_2]$, $c_2 = [MDEA]$, $c_3 = [MDEAH^+]$, $c_4 = [HCO_3^-]$, $c_5 = [OH^-]$ and $c_6 = [CO_3^{2-}]$. The liquid bulk concentration is denoted as $c_i^0(i = 1, 2, 3, \cdots, 6)$. Thus, the following equations are obtained.

Overall carbon (from CO_2) balance

$$c_1^0 + c_4^0 + c_6^0 = L \times [MDEA]_{total} \tag{6}$$

Overall MDEA balance

$$c_2^0 + c_3^0 = [MDEA]_{total} \tag{7}$$

Electroneutrality balance

$$c_3^0 = c_4^0 + c_5^0 + 2 \times c_6^0 \tag{8}$$

All reactions are at equilibrium

$$\frac{c_4^0}{c_1^0 c_5^0} = K_2 \tag{9}$$

Table 1   Model parameters for MDEA system

Parameters	Equations	Temperature range, K	References
k_1	$k_1 = 4.01 \times 10^8 \times e^{-5400/T}$	293—353	Ko and Li[9]
k_2	$\lg k_2 = 13.635 - 2895/T$	273—313	Pinsent et al.[10]
K_5	$\lg K_5 = 8909.483 - 142613.6/T +$ $4229.195 \lg T + 9.7384T - 0.0129638T^2 +$ $1.15068 \times 10^{-5}T^3 - 4.602 \times 10^{-9}T^4$	293—573	Oloffson and Hepler[11]
K_2	$\lg(K_2 K_5) = 179.648 + 0.019244T - 67.341$ $\lg T - 7495.441/T$	293—523	Simulated from the data of Read[12]
K_3	$\lg(K_3 K_5) = 6.498 - 0.0238T - 2902.4/T$	293—323	Danckwerts and Sharma[13]
K_4	$\lg(K_4 K_5) = 14.01 + 0.018T$	298—333	Barth et al.[14]
K_1	$K_1 = K_2/K_4$	293—323	
D_{MDEA}	$D_{MDEA} = 1.739 \times 10^{-9} \mu^{-0.569842}T$	not given	Hagewiesche et al.[5]

$$\frac{c_6^0}{c_4^0 c_5^0} = K_3 \qquad (10)$$

$$\frac{c_2^0}{c_3^0 c_5^0} = K_4 \qquad (11)$$

The first two reactions have finite reaction rates, which are given as follows

$$R_1 = -k_1 c_1 c_2 + \frac{k_1}{K_1} c_3 c_4 \qquad (12)$$

$$R_2 = -k_2 c_1 c_5 + \frac{k_2}{K_2} c_4 \qquad (13)$$

The following equations describe the diffusion/reaction processes

CO_2 balance

$$D_1 \nabla^2 c_1 = R_1 + R_2 \qquad (14)$$

Total carbon (from CO_2) balance

$$D_1 \nabla^2 c_1 + D_4 \nabla^2 c_4 + D_6 \nabla^2 c_6 = 0 \qquad (15)$$

Total MDEA balance

$$D_2 \nabla^2 c_2 + D_3 \nabla^2 c_3 = 0 \qquad (16)$$

Electroneutrality balance

$$D_3 \nabla^2 c_3 - D_4 \nabla^2 c_4 - D_5 \nabla^2 c_5 - 2D_6 \nabla^2 c_6 = 0 \qquad (17)$$

Instantaneous reactions (3) and (4) are assumed to be at equilibrium

$$\frac{c_6}{c_4 c_5} = K_3 \qquad (18)$$

$$\frac{c_2}{c_3 c_5} = K_4 \qquad (19)$$

The model is expressed by Eqs. (14)—(19), with the following two boundary conditions

$$c_i = c_i^0 (i = 1, 2, \cdots, 6), \quad \text{at } y = y_L \qquad (20)$$

$\nabla c_i = 0 (i = 2, 3, \cdots, 6)$, $c_1 = c_1^* = \frac{p_1}{H_1}$ when it is assumed that there is no mass transfer resistance in the gas phase, at

$$y = 0 \qquad (21)$$

The expressions of some model parameters are given in Table 1.

The nitrous oxide analogy method is used to estimate the CO_2 solubility (H_1) and the diffusivity (D_1)[15] in the aqueous solution of MDEA. The viscosity of MDEA solution can be obtained from the work of Al-Ghawas et al.[5], and the diffusion coefficients of other ionic species are assumed to be equal to that of MDEA [5].

At $T = 318 K$, some parameters from Glasscock and Rochelle[4] are used to compare our results with the solutions obtained by the code DASSL[4].

3   NUMERICAL SOLUTIONS FOR THE MODEL

3.1   Shooting method

Shooting is one of the techniques that have been widely used for boundary value problems [16]. We can reduce second order differential equations (14) and (15) to first order ones by introducing the variable $V = [v_1, v_2, v_3]^T$. And the differential equations (16) and (17) can be transformed to algebraic equations with the boundary conditions. Thus, the model can be represented as

$$\begin{cases} \nabla [c_1, c_4, c_6]^T = V \\ D_1 \nabla v_1 = R_1 + R_2 \\ D_1 \nabla v_1 + D_4 \nabla v_2 + D_6 \nabla v_3 = 0 \\ D_2 c_2 + D_3 c_3 = D_2 c_2^0 + D_3 c_3^0 \\ D_3 c_3 - D_4 c_4 - D_5 c_5 - 2D_6 c_6 = \\ \quad D_3 c_3^0 - D_4 c_4^0 - D_5 c_5^0 - 2D_6 c_6^0 \\ c_6 - K_3 c_4 c_5 = 0 \\ c_2 - K_4 c_3 c_5 = 0 \end{cases} \qquad (22)$$

For given $X = [v_1^0, v_2^0, v_3^0]^T$ (the value of V at $y = y_L$), we can get W^* (the value of $W = [c_1, v_2, v_3]^T$ at $y = 0$) by solving the initial-value problem (22).

Since $\boldsymbol{W}^*$ is dependent on $\boldsymbol{X}$, it is necessary to find out the solution $\boldsymbol{X}$ of Eq. (23) to make Eq. (22) satisfy the boundary conditions Eqs. (20) and (21).

$$f(\boldsymbol{X}) = \boldsymbol{W}^* - \left[\frac{p_1}{H_1}, 0, 0, \right]^{\mathrm{T}} = 0 \qquad (23)$$

The equation above can be solved by Newton method

$$\boldsymbol{X}^{(k+1)} = \boldsymbol{X}^{(k)} - Df[\boldsymbol{X}^{(k)}]^{-1}f[\boldsymbol{X}^{(k)}], \quad k = 0, 1, 2 \cdots \qquad (24)$$

where $Df[\boldsymbol{X}^{(k)}]$ is the Jacobi matrix of $f[\boldsymbol{X}^{(k)}]$, and its element can be approximately expressed as

$$\frac{\partial f_i[\boldsymbol{X}^{(k)}]}{\partial x_j}$$
$$\approx \frac{f_i[x_1^{(k)}, x_2^{(k)}, \cdots, x_j^{(k)}, \cdots] - f_i[x_1^{(k-1)}, x_2^{(k-1)}, \cdots, x_j^{(k-1)}, \cdots]}{x_j^{(k)} - x_j^{(k-1)}}$$
$$(i, j = 1, 2, 3) \qquad (25)$$

These procedures are accomplished by using Matlab R12 given in Fig. 1. The solution of the model by using shooting method is illustrated in Fig. 2.
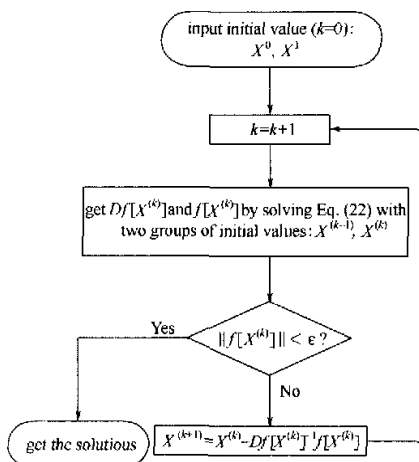

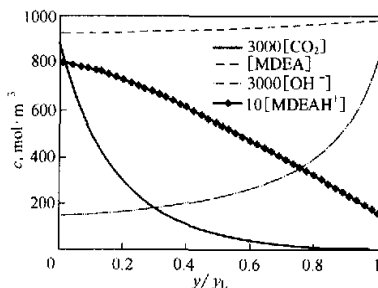
Figure 1   Flow chart for simulation with shooting method

Figure 2   Concentration profile for MDEA system with the film theory solution
$(T = 298\,\mathrm{K},\ k_{\mathrm{L}}^0 = 1.5 \times 10^{-5}\,\mathrm{m \cdot s^{-1}},\ L = 0.01;$
$c_1^* = 0.3\,\mathrm{mol \cdot m^{-3}},\ [\mathrm{MDEA}]_{\mathrm{total}} = 1000\,\mathrm{mol \cdot m^{-3}})$

3.2 Difference method

We divide the interval $[0, y_{\mathrm{L}}]$ by N parts to discretize the differential equations

$$h = \frac{y_{\mathrm{L}}}{N}, \quad y_i = jh \quad (j = 0, 1, 2, \cdots, N)$$
$$\frac{c_{i,j} - c_{i,j-1}}{h} \approx c'_{i,j},$$
$$\text{or } \frac{c_{i,j+1} - c_{i,j}}{h} \approx c'_{i,j} \ (j = 1, 2, \cdots, N) \qquad (26)$$

Equation (22) can be transformed to corresponding difference equations at jth point, if the derivative of $c_{i,j}$ is replaced by Eq. (26) ($c_{i,j}$ is the value of c_i at the jth point, $j = 1, 2, 3, \cdots, N$), the boundary conditions are given as

$$\begin{cases} c_{i,N} = c_i^0 (i = 1, 2, \cdots, 6) \\ c_{1,0} = \dfrac{p_1}{H_1} \\ v_{2,0} = 0 \\ c_{3,0} = 0 \end{cases} \qquad (27)$$

Consequently, we have $9 \times N + 9$ algebraic equations, which can be solved by Newton method. The concentration profiles of some chemical species are given in Fig. 3 when the interfacial concentration of CO_2 is $0.3\,\mathrm{mol \cdot m^{-3}}$ and $3.0\,\mathrm{mol \cdot m^{-3}}$ respectively. It can be found from Figs. 2 and 3 that the results of shooting method and difference method meet fairly well under the same condition.
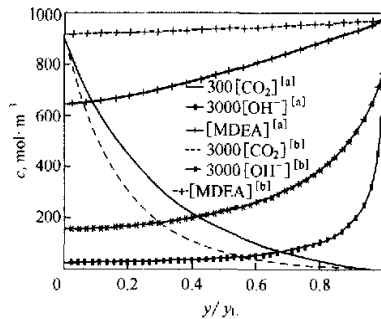

Figure 3   Concentration profile at two interfacial concentrations CO_2
$(T = 298\,\mathrm{K},\ k_{\mathrm{L}}^0 = 1.5 \times 10^{-5}\,\mathrm{m \cdot s^{-1}},\ L = 0.01;$
$[\mathrm{MDEA}]_{\mathrm{total}} = 1000\,\mathrm{mol \cdot m^{-3}})$
[a]: $c_1^* = 3.0\,\mathrm{mol \cdot m^{-3}}$; [b]: $c_1^* = 0.3\,\mathrm{mol \cdot m^{-3}}$;

Since $\nabla c_1\big|_{y=0}$ can be obtained from the concentration profile of CO_2, we illustrate the effect of CO_2 interfacial concentration on enhancement factor(E) in Fig. 5 according to Eq. (28).

$$E = \frac{N_{CO_2}}{k_{\mathrm{L}}^0(c_1^* - c_1^0)} \approx \frac{-D_1 \cdot \nabla c_1\big|_{y=0}}{k_{\mathrm{L}}^0 \cdot c_1\big|_{y=0}} = \frac{D_1}{k_{\mathrm{L}}^0}\left(\frac{\nabla c_1}{c_1}\right)_{y=0} \qquad (28)$$

Other concentration profiles (Fig. 4) are also obtained with the parameters from Glasscock et al.[4]. Figs. 4 and 5 show an excellent agreement between this work and the solutions given by DASSL[4].
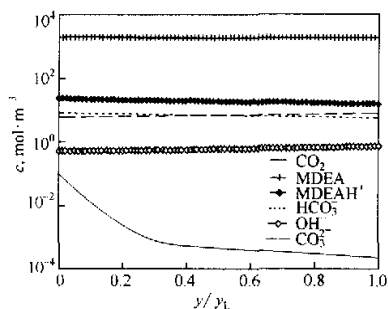

Figure 4　Concentration profile for MDEA system
$(T = 318\,\mathrm{K},\ k_L^0 = 1.46 \times 10^{-5}\,\mathrm{m \cdot s^{-1}},\ c_1^* = 0.1\,\mathrm{mol \cdot m^{-3}},$
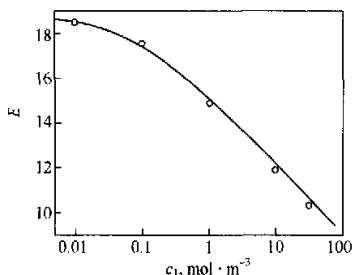$L = 0.005,\ [\mathrm{MDEA}]_{\mathrm{total}} = 2000\,\mathrm{mol \cdot m^{-3}})$

Figure 5　Effect of CO_2 interfacial concentration for the MDEA system
$(T = 318\,\mathrm{K},\ L = 0.005,\ k_L^0 = 1.46 \times 10^{-5}\,\mathrm{m \cdot s^{-1}},$
$[\mathrm{MDEA}]_{\mathrm{total}} = 2000\,\mathrm{mol \cdot m^{-3}})$
——— this work; ○ Glasscock et al.[4]

4 CONCLUSIONS

(1) The concentration profiles given by the shooting method and the difference method agree well under the same condition. And the effect of interfacial concentration of CO_2 on enhancement factor is the same as that given by Glasscock et al.[4]. These results show that the methods of shooting and difference are available for solving the rigorous model. And they provide a reliable way to understand the absorption of CO_2 by aqueous solution of MDEA. However, further experiments are necessary to determine whether film model represents reasonably well the process of absorption.

(2) The shooting method and difference method both lead to a set of nonlinear algebraic equations. It is indicated that the arbitrary initial values have a great effect on stability of these equations when Newton method is used. However, we can use modified Newton method, or choose a suitable difference equation and step to reduce the dependence on the initial values at some cases.

(3) For an unsteady-state model $\left(\dfrac{\partial c_i}{\partial t} = -D_i \dfrac{\partial^2 c_i}{\partial y^2}\right)$, a discretization technique, such as $\dfrac{\partial c_i}{\partial t} \approx \dfrac{c_{i,j} - c_{i,j-1}}{\tau}$, can be applied to transform the unsteady-state model into a steady-state one. In a sense, the techniques discussed in this paper may reveal new insights in solving the models based on penetration and surface renewal theories.

NOMENCLATURE

c	concentration of species i in the liquid phase, $\mathrm{mol \cdot m^{-3}}$
c_i	concentration of species i in the liquid phase, $\mathrm{mol \cdot m^{-3}}$
c_1^*	interfacial concentration of CO_2, $\mathrm{mol \cdot m^{-3}}$
D_i	diffusion coefficient of species i in the aqueous MDEA solution, $\mathrm{m^2 \cdot s^{-1}}$
E	enhancement factor
H_1	Henry's law constant for CO_2, $\mathrm{Pa \cdot m^3 \cdot mol^{-1}}$
h	distance step in the liquid
K_i	equilibrium constant for reaction i
k_i	rate coefficient of reaction i, $\mathrm{m^3 \cdot mol^{-1} \cdot s^{-1}}$
k_L^0	mass transfer coefficient in liquid phase, $\mathrm{m^2 \cdot s^{-1}}$
L	CO_2 loading of the aqueous MDEA solution, $\mathrm{mol \cdot mol^{-1}}$ (based on $[\mathrm{MDEA}]_{\mathrm{total}}$)
$[\mathrm{MDEA}]_{\mathrm{total}}$	total concentration of MDEA, $\mathrm{mol \cdot m^{-3}}$
N	number of points between interval $[0, y_L]$
N_{CO_2}	absorption rate of CO_2 per unit interfacial area, $\mathrm{mol \cdot m^{-2} \cdot s^{-1}}$
p_1	partial pressure of CO_2, Pa
R_i	reaction rate of reaction i, $\mathrm{mol \cdot m^{-3} \cdot s^{-1}}$
T	absolute temperature, K
t	time, s
y	distant variable
y/y_L	dimensionless distance from the interface
∇	first order differential operator, $\dfrac{\mathrm{d}}{\mathrm{d}y}$
∇^2	second order differential operator, $\dfrac{\mathrm{d}^2}{\mathrm{d}y^2}$
ε	the given precision
τ	step of time, s
μ	viscosity of MDEA solution, $\mathrm{Pa \cdot s}$

Superscripts

k	number of iteration
0	at $y = y_L$
*	at $y = 0$

Subscripts

i	chemical species
j	designation of the point in $[0, y_L]$

REFERENCES

1 Perry, R.H., Pigford, R.L., "Kinetics of gas-liquid reactions simultaneous absorption and chemical reaction", *Ind. Eng. Chem.*, **45** (6), 1247—1253 (1953).

2 Cornelisse, R., Beenackers, A.A.C.M., van Beckum, F.P.H., van Swaaij, W.P.M., "Numerical calculation of simultaneous mass transfer of two gases accompanied by complex reversible reactions", *Chem. Eng. Sci.*, **35** (5), 1245—1260 (1980).

3 Versteeg, G.F., Kuipers, J.A.M, van Beckum, F.P.H., van Swaaij, W.P.M., "Mass transfer with complex reversible

chemical reactions-I. Single reversible chemical reaction", *Chem. Eng. Sci.*, **44** (11), 2295—1310 (1989).

4 Glasscock, D.A., Rochelle, G.T., "Numerical simulation of theories for gas absorption with chemical reaction", *AIChE. J.*, **35** (8), 1271—1281 (1989).

5 Hagewiesche, D.P., Ashour, S.S., Al-ghawas, H.A., Sandall, O.C., "Absorption of carbon dioxide into aqueous blends of monoethanolamine and *N*-methyldiethanolamine", *Chem. Eng. Sci.*, **50** (7), 1071—1079 (1995).

6 Rinker, E.B., Ashour, S.S., Sandall, O.C., "Absorption of carbon dioxide into aqueous blends of diethanolamine and methyldiethanolamine", *Ind. Eng. Chem. Res.*, **39** (11), 4346—4356 (2000).

7 Petzold, L.R. A Description of DASS: A Differential/Algebraic System Solver, Sandia Report, SAND82—8637, Sandia national lab., California (1982).

8 Brenana, K.E., Campbell, S.L., Petzold, L.R., Numerical Solution of Initial-Value Problems in Differential Algebraic Equations, North-Holland, New York (1989).

9 Jiun-Jie Ko, Meng-Hui Li, "Kinetics of Absorption of Carbon Dioxide into Solutions of *N*-Methyldiethanolamine + water", *Chem. Eng. Sci.*, **55** (19), 4139—4147 (2000).

10 Pinsent, B.R.W., Pearson, L., Roughton, F.J.W., "The kinetics of combination of carbon dioxide with hydroxide ions", *Trans. Faraday Soc.*, **52** (2), 1512—1520 (1956).

11 Oloffson, G., Hepler, L.G., "Thermodynamics of ionization of water over wide ranges of temperature and pressure", *J. Solution Chem.*, **4** (2), 127—143 (1975).

12 Read, A.J., "The first ionization constant of carbonic acid form 25 to 250 ℃ and to 2000 bar", *J. Solution Chem.*, **4** (1), 53—70 (1975).

13 Danckwerts, P.V., Sharma, M.M., "The absorption of carbon dioxide into solutions of alkalis and amines(with some notes on hydrogen sulphide and carbonyl sulphide)", *Chem. Engineer.*, **44** (3), 244—280 (1966).

14 Barth, D., Tondre, C., Lappai, G., Delpuech, J. J., "Kinetic study of carbon dioxide reaction with tertiary amines in aqueous solutions", *J. Phys. Chem.*, **85** (24), 3660—3667 (1981).

15 Al-Ghawas, H.A., Hagewiesche, D.P., Gabriel Ruiz-Ibanez, Sandall, O.C., "Physicochemical properties important for carbon dioxide absorption in aqueous methyldiethanolamine", *J. Chem. Eng. Data*, **34** (1), 385—391 (1989).

16 Jiang, Ch.G., Scientific Calculation and Its Implementation in C Language, University of Science & Technology of China Press, Hefei (1998). (in Chinese)

MDEA吸收CO2稳态模型的数值求解方法

作者： 钟战铁， 李伟， 施耀， 何锋， 周明华

作者单位： Department of Environmental Engineering, Zhejiang University, Hangzhou 310027, China

参考文献(16条)

1. Perry R H. Pigford, R L Kinetics of gas-liquid reactions simultaneous absorption and chemical reaction 1953(06)

2. Cornelisse R. Beenackers, A A C M. van Beckum, F P H. van Swaaij, W P M Numerical calculation of simultaneous mass transfer of two gases accompanied by complex reversible reactions 1980(05)

3. Versteeg G F. Kuipers J A M. van Beckum, F P H. van Swaaij, W P M Mass transfer with complex reversible chemical reactions-I. Single reversible chemical reaction 1989(11)

4. Glasscock D A. Rochelle, G T Numerical simulation of theories for gas absorption with chemical reaction 1989(08)

5. Hagewiesche D P. Ashour, S S. Al-ghawas, H A. Sandall,O C Absorption of carbon dioxide into aqueous blends of monoethanolamine and N-methyldiethanolamine 1995(07)

6. Rinker E B. Ashour, S S. Sandall, O C Absorption of carbon dioxide into aqueous blends of diethanolamine and methyldiethanolamine 2000(11)

7. Petzold L R A Description of DASS: A Differential/Algebraic System Solver, Sandia Report, SAND82-8637 1982

8. Brenana K E. Campbell, S L. Petzold, L R Numerical Solution of Initial-Value Problems in Differential Algebraic Equations 1989

9. Jiun-Jie Ko. Meng-Hui Li Kinetics of Absorption of Carbon Dioxide into Solutions of N-Methyldiethanolamine +water 2000(19)

10. Pinsent B R W. Pearson,L. Roughton,F J W The kinetics of combination of carbon dioxide with hydroxide ions 1956(02)

11. Oloffson G. Hepler L G Thermodynamics of ionization of water over wide ranges of temperature and pressure 1975(02)

12. Read A J The first ionization constant of carbonic acid form 25 to 250 ℃ and to 2000 bar 1975(01)

13. Danckwerts P V. Sharma, M M The absorption of carbon dioxide into solutions of alkalis and amines(with some notes on hydrogen sulphide and carbonyl sulphide) 1966(03)

14. Barth D. Tondre, C. Lappai, G. Delpuech, J J Kinetic study of carbon dioxide reaction with tertiary amines in aqueous solutions 1981(24)

15. Al-Ghawas H A. Hagewiesche D P. Gabriel RuizIbanez. Sandall, O C Physicochemical properties important for carbon dioxide absorption in aqueous methyldiethanolamine 1989(04)

16. Jiang Ch G Scientific Calculation and Its Implementation in C Language 1998

相似文献(10条)

1.外文期刊 ZHONG Zhantie.LI Wei.SHI Yao.HE Feng.ZHOU Minghua A New Method to Solve Film Model for CO_2 Absorption with Aqueous Solution of N-Methyldiethanolamine

The shooting method and the difference method are used for numerical simulation of CO_2 absorption with aqueous solution of methyldiethanolamine (MDEA). It is demonstrated that these methods are available for the steady-state model, which may be expressed as a set of differential algebraic equations (DAEs) with two-point boundary values. This method makes it possible not only to obtain the concentration profiles for MDEA system, but also to reveal the effect of CO_2 interfacial concentration on the enhancement factor. With this numerical simulation, the mass transfer process with multicomponent diffusion and reactions can be better understood.

2.外文期刊 Hiroshi Suzuki.Tomofumi Yamanaka.Wataru Nagamoto.Takahide Sugiyama Modeling of liquid film along absorber cylinders in an absorption chiller

A two-dimensional liquid film model of LiBr solution falling along absorber cylinders has been studied to obtain boundary conditions for computing vapor flow in the absorber-evaporator of an absorption chiller. The model was established based on the assumptions that LiBr concentration and temperature profiles in the liquid film obey the third order polynomial expressions. It was indicated that mass flux and absorbed heat on the liquid surface can be calculated with simple numerical computations on the present analytical model. The overall heat transfer coefficient and total absorbed mass per second calculated with the present liquid film model was compared with experimental data for validation. The results calculated with the present model showed good agreement with the experimental data. Then, it was concluded the present model was useful enough for determining surface conditions on the LiBr liquid film around absorber cylinders.

3.外文会议 Chao-Hui Zhang.Shi-Zhu Wen.Jian-Bin Luo Lubrication Theory for Thin Film Lubrication Accounting for the Ordered Film Model

In this paper, the features in thin film lubrication (TFL) are investigated with the use of nematic theory accounting for the ordered film. In TFL, in which dominated by the ordered molecules, the alignments of molecules can roughly be described by a unit vector, the director, and then the phenomena can be construed accordingly. The fundamental continuum flow theory is applied to the two-dimensional lubrication geometry. The angular distribution profile is solved from the angular momentum equation which couples the viscosity and elastic effects. Other than in nematic case, in which the Leslie coefficients are the properties of lubricant, the Leslie coefficients are determined by the combination of solid walls and the lubricants in TFL. A parameter named as viscosity-to-elasticity ratio is introduced to account for the relative effect of viscosity to elasticity.

4.外文期刊 Maurizio BOTTOM Molecular Approach to Sodium Vapour Condensation, Rewetting and Vaporization in LMFBR Bundle under Hypothetical Accident Conditions

In the frame of safety analysis of Liquid Metal Fast Breeder Reactors (LMFBRs) under hypothetical Unprotected Loss-of-Flow (ULOF) conditions, two phase flow of sodium is simulated in a reactor core. Traditional approaches used in safety analysis codes to simulate sodium vapour condensation and vaporization rely upon application of macroscopic semi-empirical correlations for heat transfer and vapour condensation or evaporation rates. As an alternative to this macroscopic approach, we developed a microscopic methodology based upon the application of the basic laws of the kinetic theory for the determination of the evaporation and condensation rates of vapour in a reactor bundle. This microscopic approach is based upon a Monte Carlo simulation of the molecular trajectories, collision rates between vapour molecules and of the molecules with the surfaces of the claddings of the pins of a reactor bundle. The pins surfaces are treated in the Monte Carlo simulation as diffusely reflecting surfaces. Scattering of sodium particles is simulated with the "hard sphere" collision model. The "step splitting" technique is applied, which consists in separating the collisions dynamic calculation from collisionless paths of the molecules. Vapour particles are assumed to condense on the surfaces of the pins when, after diffuse reflection, their velocity would be less than one third of the most probable velocity corresponding to the wall temperature. Rewetting of dried out regions of the cladding surfaces is simulated with a dynamic film model which computes the velocity distribution of the liquid across the film thickness and then the mean liquid film velocity. Evaporation of sodium molecules from the film yields a source of molecules which re-enter into the Monte Carlo calculation of the molecular dynamic approach. The coupling of the micro- and macroscopic models has been applied to the numerical simulation of an out-of pile sodium boiling experiment run at the Nuclear Research Cent

5.外文期刊 Feng. YH.Qu. JP.He. HZ.Jin. G.Cao. XW.Song. J Simulation of nonisothermal flow of melt during melting process of vibration-induced polymer extruder

A simplified 2D melt film model was established to simulate the nonisothermal melt flow during the melting process of the vibration-induced polymer extruder of which the screw can vibrate axially. Since polymer has time-dependent nonlinear viscoelastic characteristic with vibration force filed (VFF), a self-amended nonisothermal Maxwell constitutive equation that can reflect the relaxation time spectrum of polymer was adopted. Using the 2D melt film model, melt films of two kinds of thickness representing different melting stages were simulated to investigate the influence tendency of the same VFF on the different melting stage. Special flow patterns and temperature distribution of melt in the melt film between the driving wall and the solid/melt interface with various vibration force fields were systematically simulated. It is found out that within a certain range of vibration strength, the application of vibration can optimize the time-averaged shear-rate distribution, improve the utilization efficiency of energy, and promote melting process; and the thinner the melt film is, the more intense the nonlinear viscoelastic response becomes with the same VFF; moreover, there exists optimum vibration strength to make the melting process fastest, which is in accord with the visualization experimental results. (c) 2006 Wiley Periodicals, Inc.

6.外文会议 Hui Ma.Hong Liang Yao.Zhao Hui Ren.Feng Wen.Bang Chun Wen NUMERICAL SIMULATION AND EXPERIMENTAL RESEARCH ON PEDESTAL LOOSENESS OF A ROTOR SYSTEM

The mechanical model of looseness of fastening bolt on the bearing pedestal is set up based on the project practice. Using the

nonlinear oil-film model put forward by Adiletta, the dynamic characteristics were investigated by numerical Runge-Kutta method. At last, the experiment is performed to investigate the pedestal looseness by a test rig and the fault signals are analyzed by the spectrum cascade and reassigned wavelet scalogram. Numerical simulation and experiment all show that system motion state changes frequently with the increase of the rotating speed. And the experimental results coincide with the simulation results.

7. 外文会议 Hui Ma. Hong Liang Yao. Zhao Hui Ren. Feng Wen. Bang Chun Wen NUMERICAL SIMULATION AND EXPERIMENTAL RESEARCH ON PEDESTAL LOOSENESS OF A ROTOR SYSTEM

The mechanical model of looseness of fastening bolt on the bearing pedestal is set up based on the project practice. Using the nonlinear oil-film model put forward by Adiletta, the dynamic characteristics were investigated by numerical Runge-Kutta method. At last, the experiment is performed to investigate the pedestal looseness by a test rig and the fault signals are analyzed by the spectrum cascade and reassigned wavelet scalogram. Numerical simulation and experiment all show that system motion state changes frequently with the increase of the rotating speed. And the experimental results coincide with the simulation results.

8. 外文期刊 R. Greef. J. G. Frey. J. Robinson. L. Danos Adsorption of rhodamine 6G at the water-air interface

We wanted to detect and quantify adsorption of Rhodamine 6G (R6G) at the air/water interface to supplement previous work using second harmonic generation [1-4]. We found that at incidence angles close to the Brewster angle this can be achieved, even at very low bulk concentration. Fitting to a single film model, we found that adsorption can be measured down to very low concentrations of $10^{(-7)}$M. This is contrasted with the behaviour of other dyes and other solvents. Outside the wavelength range of the dye absorption band the refractive index of the surface approaches that of pure water.

9. 外文期刊 Hiroshi SUZUKI. Wataru NAGAMOTO. Takahide SUGIYAMA Simulation on Vapor Flow in the Absorber/Evaporator of an Absorption Chiller

Two-dimensional numerical computation methodology for vapor flow in the absorber/evaporator in an absorption chiller has been suggested and the effect of pitch ratio of cylinders in the absorber/evaporator has been discussed. Pseudo-diffusion effects of surfactants added to lithium bromide solution flowing along cylinders in the absorber were considered into liquid film model suggested in the previous study. From the results, the present model was found to agree well with experimental data in a rather wide range of the pressure in the present system. The present model effectively reduces the computational load for vapor flow in the absorber/evaporator including 176 cylinders. Near the top and bottom walls of the absorber/evaporator, the high velocity regions were observed and the recirculating regions were also found to be formed just inside of the high velocity regions, This high velocity region is intensified with pitch-to-diameter ratio decrease because the vapor flow penetrating from the back side of the absorber increases for the pressure drop increase of front side of the absorber.

10. 外文会议 Nicolas Kruse. Kuo-Huey Chen Exterior Water Management Using a Custom Euler-Lagrange Simulation Approach

The reduction of hardware vehicle models during development drives the necessity to transfer most hardware tests to VR Simulation. Exterior water management is one of the topics, where complex physics meet everyday situations. A vehicle contamination test conducted in a wind tunnel is selected to be transferred to numerical simulation. The method of choice is the Euler-Lagrange approach with modeled "liquid" wall particles. A new wall film model has been developed in the present study to include the observed liquid properties in physical test. This model takes the local wetting conditions into account and constitutes a reformulation of the local force balance of the wall liquid. Also the wall film separation model has been refined and improved. With this new approach, the gas/liquid, liquid/solid and liquid/liquid interaction has been remodeled. The application of the custom Euler-Lagrange Simulation Approach to the selected contamination test procedure proves the practicability to generally resemble the spread of liquid over a vehicle observed in physical tests by numerical simulation.

引证文献(1条)

1. 徐霖. 沈喜洲 胺溶液脱碳的研究现状及发展趋势 [期刊论文] - 化学与生物工程 2006(12)